Applied Catalysis B: Environmental 197 (2016) 138–145

Contents lists available at ScienceDirect

Applied Catalysis B: Environmental

journal homepage: www.elsevier.com/locate/apcatb

Hydrogen production from hydrocarbons over Rh supported on Ce-based oxides for automotive applications

S. Rijo Gomes, N. Bion, D. Duprez, F. Epron*

Université de Poitiers, CNRS UMR 7285, Institut de Chimie des Milieux et Matériaux de Poitiers (IC2MP), 4 rue Michel Brunet, TSA 51106, 86073 Poitiers Cedex 9, France

ARTICLE INFO

Article history:
Received 27 November 2015
Received in revised form 6 January 2016
Accepted 10 January 2016
Available online 13 January 2016

Keywords:
Hydrogen production
Catalytic fuel reforming
Ceria-based supports
Rhodium

ABSTRACT

On-board hydrogen production by reforming of fuel in the exhaust gas recirculation loop allows increasing the engine yield, thus decreasing the fuel consumption, and the formation of pollutants such as NOx. Various catalysts based on Rh supported on cerium-based oxides with alumina were prepared and characterized. Their catalytic performances were evaluated in the reforming of isooctane, chosen as model molecule, in the presence of a gas mixture of composition representative of the exhaust gas, i.e. H_2O, CO_2, O_2 and N_2. It was shown that the best performances in terms of hydrogen yield were obtained with the supports containing both ceria, in high amounts, and alumina, due to the high thermal stability of the support, the high metal dispersion and the limited sintering.

1. Introduction

In vehicles Exhaust Gas Recirculation (EGR) technique was initially developed for decreasing the temperature in the combustion chamber to limit NOx production in Diesel engines. It is now commonly used for gasoline engines with direct injection spark ignition working in lean burn conditions, for which the conventional three way catalysts cannot work efficiently. EGR also reduces throttling losses in gasoline engine, and consequently fuel consumption [1]. On-board Hydrogen production by reacting fuel with exhaust gas [2–7] in the presence of a catalyst process may enhance the efficiency of EGR systems. In this process, schematized in Fig. 1, hydrogen is virtually produced by reaction of hydrocarbons with the main components of the exhaust gas, CO_2 and H_2O, by dry and steam reforming, respectively. These two reactions being endothermic, this allows to recover energy from the exhaust gas [7]. Other reactions, such as total, partial oxidation or water-gas-shift reactions may also occur but their contribution is minority in the whole process [7]. Small amount gasoline may be added in the system to increase the amount of hydrogen produced. The combustion in the engine with a gas enriched in H_2, by this process named Reforming of Exhaust Gas Recirculation (REGR), increases the ratio H/C of the fuel, decreasing the production of CO and the fuel consumption by an increase of combustion efficiency [2,7,8].

Rhodium-based mono or bimetallic catalysts have proven their efficiency for producing hydrogen in the REGR conditions [9–11], i.e. in the presence of a fuel, water, CO_2, O_2 and N_2. In the REGR conditions, mainly steam and dry fuel reforming may occur. We have shown [12] that Rh (1 wt%) supported on zirconia doped with 26.2 wt% of a mixture of La_2O_3, Nd_2O_3 and Y_2O_3 (ZLNY support) exhibited high activity for REGR gasoline process application, using isooctane (C_8H_{18}) as a model molecule. Despite a partial C_8H_{18} conversion, high H_2 yields were obtained, with CH_4 yields lower than those predicted at the thermodynamic equilibrium. The study (i) on the effect of water, CO_2 and REGR condition, i.e. the study of the steam reforming, dry reforming and REGR reactions separately, in various conditions of temperature and contact time and (ii) on the conversion of methane and its production by CO or CO_2 methanation, or by C_8H_{18} hydrogenolysis or decomposition, enabled us to propose a reaction scheme in 3 successive steps for isooctane conversion in REGR conditions, i.e. the reforming of isooctane in the presence of water, carbon dioxide and oxygen [13], yielding H_2 and CO_2, CO and CH_4:

Step 1, corresponding to reforming reactions i.e. steam reforming (Eq. (1)) and dry reforming (Eq. (2)) yielding H_2 and mainly CO_2, dry reforming reaction being negligible:

$$C_8H_{18} + 16H_2O \rightarrow 8CO_2 + 25H_2 \quad (1)$$

$$C_8H_{18} + 8CO_2 \rightarrow 16CO + 9H_2 \quad (2)$$

* Corresponding author.
E-mail address: florence.epron@univ-poitiers.fr (F. Epron).

http://dx.doi.org/10.1016/j.apcatb.2016.01.022
0926-3373/

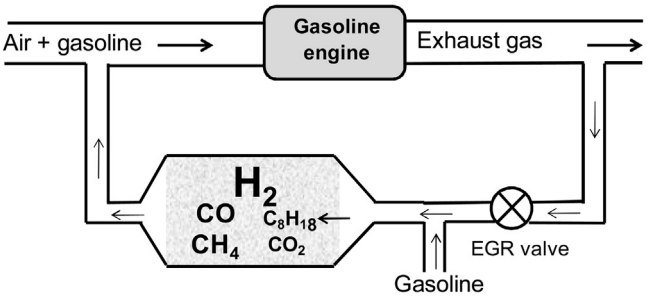

Fig. 1. Scheme of the REGR process.

Step 2, corresponding to the reverse water gas shift (RWGS) reaction, yielding CO:

$$CO_2 + H_2 \leftrightarrow CO + H_2O \quad (3)$$

Step 3, corresponding to methanation reactions, especially with CO, yielding CH_4:

$$2CO + 2H_2 \leftrightarrow CH_4 + CO_2 \quad (4)$$

The partial and total oxidation reactions were negligible, except for low isooctane conversions, due to the small amount of O_2 in the gas phase compared to those of H_2O and CO_2 in REGR reaction. A slight deactivation was observed, which was attributed to either the metal sintering or a poisoning of the Rh/support interface.

The stability of reforming catalysts depends strongly on the nature of the support and on the metal-support interactions. Ceria-based supports present interesting properties for reforming reactions since (i) ceria favors strong metal-support interactions, thus limiting metal sintering [14] and (ii) is able to release oxygen and reduce its valence from Ce^{4+} to Ce^{3+} in oxygen-poor environments, and re-oxidize in oxygen-rich environments, which helps preventing deactivation by coke deposition [15].

In the present study, production of hydrogen from isooctane will be investigated in the presence of rhodium catalysts supported on cerium-based oxides with alumina in REGR conditions, as the previous ones [12,13]. Alumina was added to improve the stability of the ceria based support. The supports will be CeO_2–Al_2O_3, which has demonstrated high ceria reducibility [16,17] and CeO_2–ZrO_2 (50:50)/Al_2O_3, CeO_2–ZrO_2 (50:50) presenting high oxygen mobility [18] and high performances for REGR reaction [19].

2. Experimental conditions

2.1. Catalysts

Five supports were used: γAl_2O_3, CeO_2, Al_2O_3(80%)–CeO_2(20%), Al_2O_3(20%)–CeO_2(80%), $Ce_{0.5}Zr_{0.5}O_2/Al_2O_3$(10%). In the following they will be named: Al_2O_3, CeO_2, Al(80)Ce(20), Al(20)Ce(80), these four supports corresponding to the Al(Cex) series, and CeZrAl, respectively.

Al_2O_3 was provided by Axens and CeO_2 by Solvay (Rare-earth systems). Al(80)Ce(20) was prepared by impregnation of $Ce(NO_3)_3.6H_2O$ on the commercial Al_2O_3 support in excess of water. Al(20)Ce(80) and CeZrAl were prepared by a sol-gel method adapted from Ref. [20]. After evaporation of water, supports were dried and then calcined at 800 °C in a muffle furnace for 5 h.

Rhodium (1 wt% Rh) was impregnated on the support by wet impregnation technique using rhodium(III) chloride (Alfa Aesar). After evaporation of the solvent, the as-made sample was dried, and then calcined at 650 °C, under air flow (60 cm^3 min^{-1}) for 4 h (temperature ramp: 2 °C min^{-1}).

2.2. Characterization

The specific surface area of the catalysts was estimated by the BET (Brunauer–Emmett–Teller) model using nitrogen adsorption at −196 °C in a Tristar 3000 Micromeritics apparatus. The pore size distribution was calculated using BJH (Barret-Joyner-Halenda) model.

The metal content was determined by elemental analysis using inductively coupled plasma atomic emission spectroscopy (ICP-AES) technique in a PerkinElmer Optima 2000 DV apparatus.

Rh accessibility was measured by H_2 chemisorption. Typically 120 mg of sample were reduced in flowing hydrogen at 400 °C (1 h, heating rate 10 °C min^{-1}), flushed under Ar (3 h), and then cooled down to room temperature under flowing Ar. The H_2 uptake measurements were performed at −86 °C by injecting a first series of hydrogen pulses (0.267 cm^3) up to saturation (HC1). The low temperature of chemisorption was required to suppress hydrogen spillover on the support [21]. A second series of pulses was injected over the sample, after 10 min of purging under pure Ar, to determine the reversible part of chemisorbed hydrogen (HC2). The irreversible part was taken as HC=HC1 −HC2.

Temperature Programmed Reduction (TPR) experiments were performed in a Micromeritics AutoChem II apparatus. Before analysis, the samples (~200 mg) were treated under flowing oxygen from RT to 500 °C for 30 min with the heating rate of 10 °C min^{-1}. Catalysts were then cooled down to RT under O_2 (30 mL min^{-1}) and outgassed under argon for 30 min (30 mL min^{-1}). Finally TPR was performed from RT up to 1000 °C at a rate of 5 °C min^{-1} for 30 min under 1% H_2/Ar (30 mL min^{-1}). H_2 consumption was quantified by gas chromatography using a Thermal Conductivity Detector (TCD).

X-ray diffraction measurements were performed at room temperature in a Bruker AXS D5005 X-ray diffractometer, working with CuKα radiation (λ = 1.54184 Å), generated at 40 kV and 40 mA. Signal is recorded for 2θ between 15° and 85° with a step of 0.04° and a step time of 6 s. For sample identification, diffraction patterns were compared to the ICDD (International Center for Diffraction Data) database integrated in the EVA software. The crystallite size was calculated using the Debye–Scherrer equation.

2.3. Catalytic test

The model feed of gasoline exhaust gas, given by PSA Peugeot Citroën Group, contains 2.2 vol.% of isooctane, 13.5 vol.% of CO_2, 12 vol.% of H_2O, 1 vol.% of O_2 and 71.3 vol.% of N_2 (REGR conditions). Anhydrous isooctane (C_8H_{18}) was supplied by Carlo Erba (99.5%); CO_2, O_2 and N_2 were provided by Air Liquide. Ultra pure water was used. The total gas flow rate was 250 Ncm^3 min^{-1}

Reforming of exhaust gas recirculation (REGR) reaction was carried out in a quartz tubular continuous flow reactor. The catalyst (150 mg) was activated under the REGR conditions, i.e. in the presence of all the reactants, or under hydrogen, by heating with a ramp of 10 °C min^{-1}, from 130 °C to the reaction temperature. The experiments were performed at 580 °C, with a total pressure of 1.3 bar and a weight hourly space velocity of 138 h^{-1}, which corresponds to a gas hourly space velocity of roughly 150,000 h^{-1}, considering an average density of the solids of 1.5 g mL^{-1}. The experimental details for the experiments in the tubular continuous flow reactor are given in details in Ref. [12].

The catalyst performances were characterized by:

- The product yield:

$$Y_x = \frac{F_x^{out}}{F_{C_8H_{18}}^{in}}$$

Table 1
Surface area of catalysts and supports and volume and size of pores for the supports.

Supports and catalysts	BET surface area (m^2/g)	Volume of pores (cm^3/g)	Size of pores (Å)
Al_2O_3	184	0.49	108
Rh/Al_2O_3	175	–	–
CeO_2[a]	256	0.17	147
Rh/CeO_2	42	–	–
Al(80)Ce(20)	103	0.32	124
Rh/Al(80)Ce(20)	102	–	–
Al(20)Ce(80)	34	0.07	76
Rh/Al(20)Ce(80)	29	–	–
CeZrAl	66	0.20	125
Rh/CeZrAl	57	–	–

[a] Not calcined.

where $F^{in}_{C_8H_{18}}$ is the molar flow rate of isooctane at the inlet of the reactor and F^{out}_x the molar flow rate of the product x at the outlet

- The isooctane, oxygen, carbon dioxide and water conversion, in% (example for isooctane):

$$X_{C_8H_{18}} = \frac{F^{in}_{C_8H_{18}} - F^{out}_{C_8H_{18}}}{F^{in}_{C_8H_{18}}} \times 100$$

Experimental values are compared to the values at the thermodynamic equilibrium obtained by calculation based on the minimization of the Gibbs free energy.

3. Results and discussion

3.1. Characteristics of the catalysts

The characteristics of the supports and of the catalysts in terms of surface area, volume and size of pores are reported in Table 1. Supports present BET surface area between 34 (Al(20)Ce(80)) and 256 $m^2\ g^{-1}$ (CeO_2). The introduction of rhodium, followed by activation treatments, leads to a slight decrease of the BET surface, except on CeO_2 support, for which the specific surface area significantly decreases to 42 $m^2\ g^{-1}$. This is due to the fact that the CeO_2 support was not calcined, before introduction of rhodium. When cerium is added to aluminium oxide, it can be seen (Fig. 2) that the BET surface of the Rh/AlCex catalysts decreases from 175 to less than 50 $m^2\ g^{-1}$.

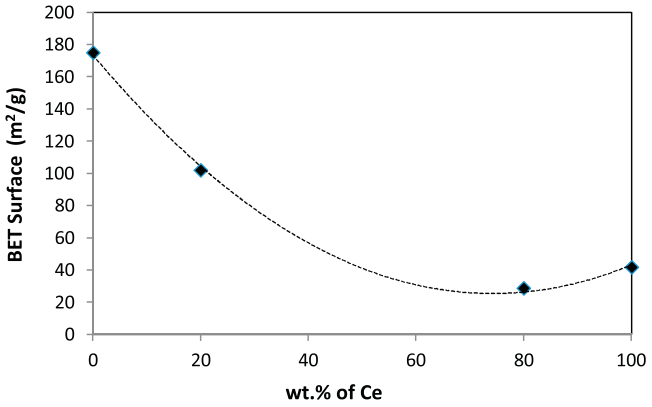

Fig. 2. Effect of the cerium content in Rh/Al(Cex) catalysts on the BET surface.

XRD patterns are displayed in Fig. 3. γ-Al_2O_3 (ICDD no. 00-029-0063) is clearly identified on the Rh/Al_2O_3 pattern. The cell parameter (a = 0.791 nm), experimentally determined from the most intense peak (2θ = 66.9°), corresponds to the (4,4,0) plane. The crystallite size is estimated at ~9.9 nm. Rh/CeO_2 presents sharp diffraction lines corresponding to cerianite ceria (ICDD no. 00-043-1002) crystallizing in a fluorite type fcc structure, with a crystallite size of 25.6 nm. Rh/Al(80)Ce(20) presents both type of ceria and alumina phases, which indicates that cerium is not incorporated in the alumina structure. The XRD pattern of Rh/Al(20)Ce(80) shows only peaks characteristic of ceria, showing that alumina is likely to be amorphous. The cell parameters of Rh/Al(80)Ce(20) and Rh/Al(20)Ce(80), are 0.539 nm and 0.540 nm, similar to ceria (cerianite), and the mean crystallite size of the pseudo-cerianite phase of 21.6 nm and 27.3 nm, respectively. Rh/CeZrAl presents diffraction lines typical of $Ce_{0.5}Zr_{0.5}O_2$ (ICDD no. 00-038-1436), showing that the alumina added to this support is amorphous and does not modify the oxide structure. In Rh/CeZrAl, CeZr is a homogeneous solid solution with a mean crystallite size of 18.7 nm, and cell parameters (a = b = 0.372 nm; c = 0.527 nm) similar to the ICDD (a = b = 0.372 nm; c = 0.530 nm).

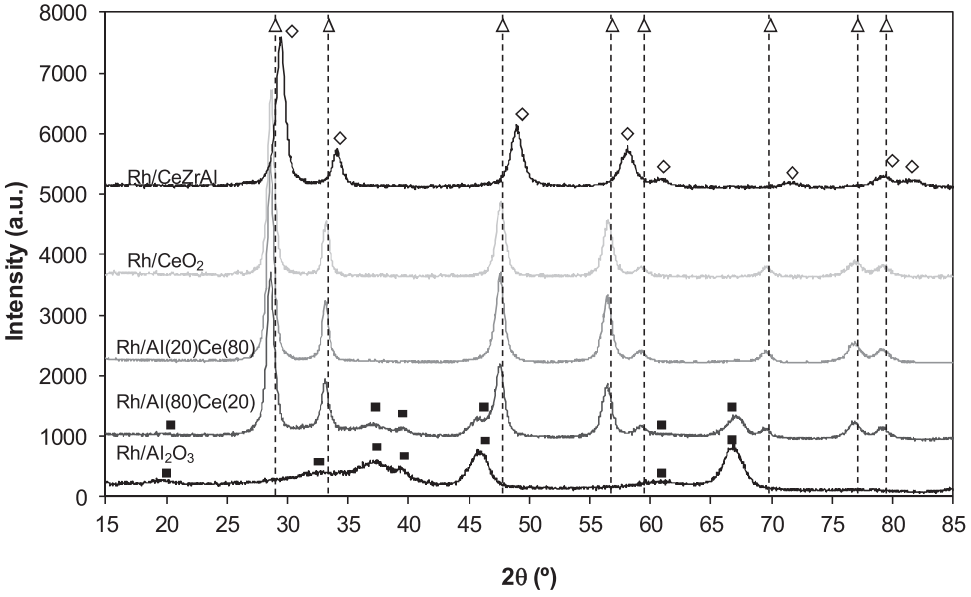

Fig. 3. X-Ray diffraction patterns of the Rh/Al(Cex) series and of the Rh/CeZrAl catalyst; (■): γ-Al_2O_3; (Δ): CeO_2; (◊): $Ce_{0.5}Zr_{0.5}O_2$.

Table 2
TPR results of Al(Cex) series and CeZrAl.

Support	CeO_2	Theo. H_2 consumption for CeO_2	T_{max}		Exp. H_2 consumption		% of reduction of surface Ce^{4+} to Ce^{3+}[a]
	(wt%)	(μmol H_2/g)	pic 1 (°C)	pic 2 (°C)	TOTAL (μmol H_2/g)	pic 1 (μmol H_2/g)	pic 1 (%)
Al_2O_3	0%	–	–	–	–	–	–
CeO_2	100%	2905	371	1025	–[b]	217	7%
Al(80)Ce(20)	20%	581	538	986	634	40	7%
Al(20)Ce(80)	80%	2324	580	990	1303	75	3%
CeZrAl	51.9%	1508	657	1088	1572	399	26%

[a] Calculated from the theoretical value.
[b] Consumption not finished at the end of the experiment.

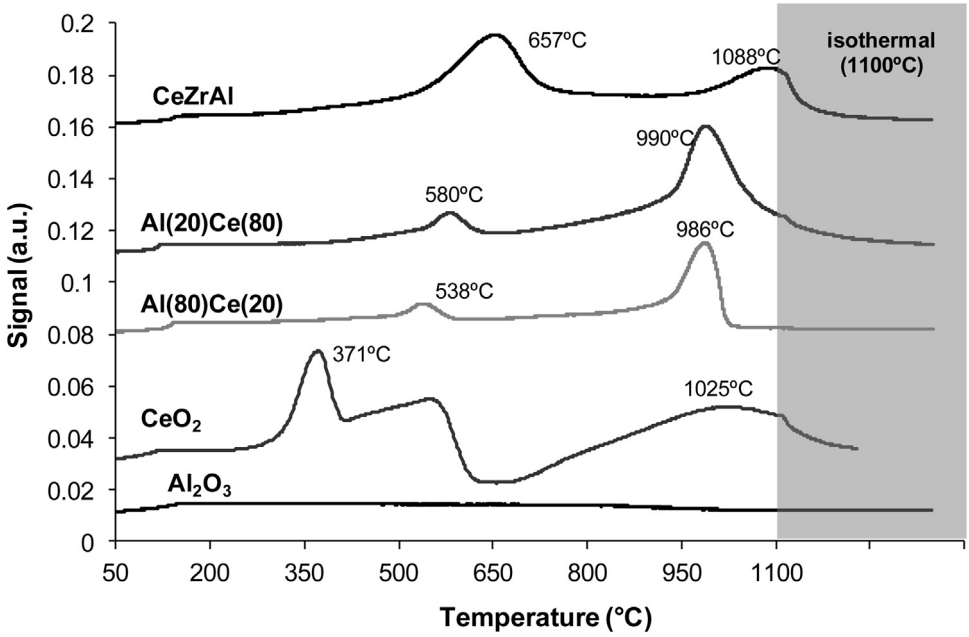

Fig. 4. TPR profiles of the Al(Cex) series and CeZrAl.

TPR profiles of the Al(Cex) series and CeZrAl, are presented in Fig. 3 and the results detailed in Table 2. No peak is observed on the alumina support, due to the non-reducibility of this support. It can be seen in Fig. 3 that CeO_2 presents a first reduction peak with a maximum at 371 °C and a second one, starting at 660 °C. The first peak may be attributed to the reduction of surface Ce^{4+}. Generally, CeO_2 presents two peaks during the reduction process: a first one, around 400 °C, attributed to surface reduction and the second one, above 750 °C, corresponding to the reduction of the bulk [22,23]. It can be seen in Table 2 that only 7% of ceria is reduced at the first peak attributed to surface ceria, which is little and may be attributed to the low temperature of this first reduction peak. Mixed Al(80)Ce(20) and Al(20)Ce(80) supports start to be reduced at temperatures higher than that of CeO_2, with a first maximum of reduction peak 538 and 580 °C, respectively, attributed to the reduction of surface ceria, and a second one at 986 and 990 °C to bulk ceria, in accordance with the results obtained by Yao et al. [22] on the same type of support. For Al(80)Ce(20), total consumption of hydrogen is similar to the theoretical one, indicating that all ceria has been reduced. On the contrary, the experimental one for Al(20)Ce(80) (1303 μmol/g) is much lower than the theoretical one, which may be explained, by the desorption of hydrogen as for pure CeO_2, or by an incomplete reduction of Ce^{4+}. For CeZrAl, two peaks are observed with maxima at 657 °C and at 1088 °C, whereas it is known that the presence of Zr allows starting the reduction of Ce^{4+} at lower temperature [24]. This different behaviour may be explained by the presence of 10 wt% of Al_2O_3 that may hinder the reduction of $Ce_{0.5}Zr_{0.5}O_2$. However, the first peak (657 °C), which may be attributed to the surface reduction, corresponds to 26% of the total consumption, which is much higher than that observed for the Al(Cex) series (3%–7%). Consequently, the first peak most probably corresponds to the reduction of ceria surface and subsurface [24]. As for Al(80)Ce(20), the reduction of CeO_2 is complete, with an experimental total H_2 consumption similar to the theoretical one.

Fig. 4 displays the TPR profile of the catalysts after impregnation of Rh(1 wt%). Compared to the bare supports (Fig. 4) the presence of the metal favours the reduction of Ce^{4+}. Two domains of temperature can be identified. In the first one (T < 350 °C), the first reduction peak in the 120–244 °C range, is attributed to the simultaneous reduction of Rh_2O_3 and of the surface ceria, the presence of the metal favouring the spillover of hydrogen towards the support. It can be seen that, except for Rh/Al(20)Ce(80) presenting the lowest temperature of reduction, the temperature of the maximum of the first peak decreases as the cerium content increases. In the second part (T > 350 °C), the reduction of bulk ceria can occur. The experimental amount of hydrogen consumed in the first domain (T < 350 °C) and H_2/Rh molar ratio are reported in Table 3 for each catalyst. Considering the total oxidation of Rh to Rh_2O_3 during the oxidizing pre-treatment, the total reduction of this oxide must correspond to a consumption of 146 μmol H_2 g^{-1}, and H_2/Rh = 1.5. Except for Rh/Al_2O_3, this molar ratio is superior to 1.5, due to the reduction of surface CeO_2 (spillover), which occurs at low temperature. This phenomenon is particularly noticeable for Rh/CeZrAl (H_2/Rh = 6.1). The low H_2 consumption for Rh/Al_2O_3 is due to the

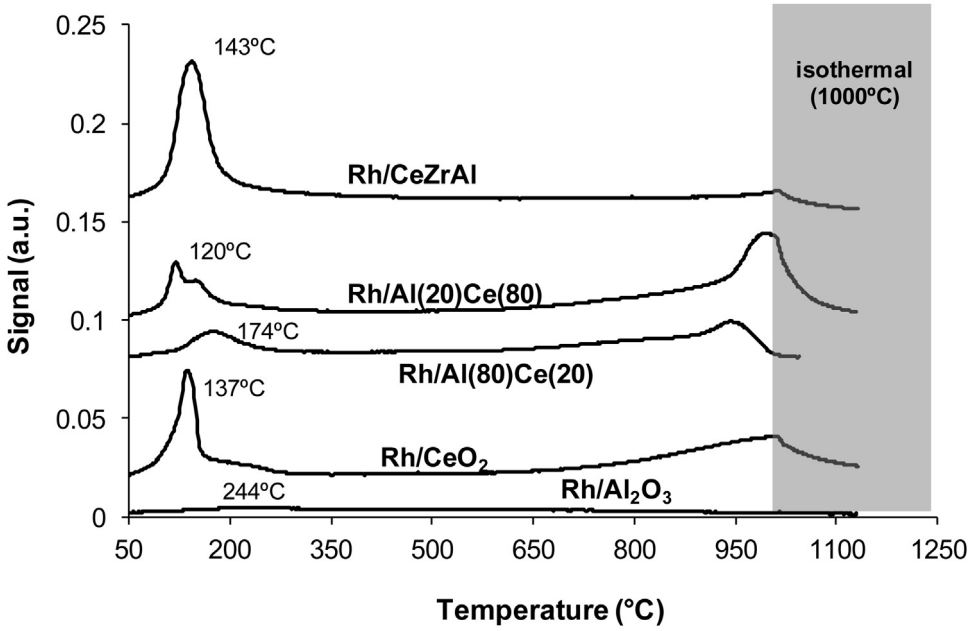

Fig. 5. TPR profiles of Rh/Al(Cex) series and Rh/CeZrAl.

Table 3
Amount of H_2 consumption and H_2/Rh molar ratio at the first reduction peak (T_{max} < 350 °C).

Reduction at T_{max} < 350 °C	Exp. H_2 cons. (μmol H_2/g)	H_2/Rh (mol/mol)
Rh/Al_2O_3	51	0.5
Rh/CeO_2	369	3.8
Rh/Al(80)Ce(20)	160	1.6
Rh/Al(20)Ce(80)	252	2.6
Rh/CeZrAl	595	6.1

Table 4
Metal content, metal dispersion and metal particle size of Rh/Al(Cex) and Rh/CeZrAl catalysts.

Catalysts	Metal content (ICP)	Dispersion[a]	Particle size[b] (Å)
Rh/Al_2O_3	1.10%	39%	24
Rh/CeO_2	1.01%	18%	51
Rh/Al(80)Ce(20)	1.09%	43%	21
Rh/Al(20)Ce(80)	1.03%	42%	22
Rh/CeZrAl	1.01%	46%	20

[a] Considering H/Rh = 1.
[b] Calculated from the dispersion value.

calcination temperature of 650 °C. It is known that, when Rh/Al_2O_3 is oxidized at temperatures higher than 600 °C, Rh^{3+} easily diffuses into the spinel structure of γAl_2O_3 and is then difficult to reduce [25–28].

All the catalysts, except Rh/CeO_2, present a metal dispersion of roughly 40%, corresponding to a particle size of ~22 Å (Table 4). The low dispersion of Rh/CeO_2 (18%) is attributed to the support sintering, which occurs during the calcination process, leading to a drastic decrease of the BET surface area (from 256 to 42 $m^2\ g^{-1}$, Table 1) (Fig. 5).

3.2. Catalytic performances

The composition of the gas phase in the reforming conditions using isooctane as model molecule are summarized in Table 5 along with the one obtained after a blank test, i.e. a reaction in the standard conditions but without any catalyst. It

Table 5
Composition of the gas in the REGR condition and of the outlet gas (blank reaction without catalyst at 580 °C, P = 1.3 bar, WHSV = 137.8 h^{-1}).

Component	Inlet composition (mol.%)	Inlet composition (mol/mol C_8H_{18})	Products after blank reaction (mol/mol C_8H_{18})
C_8H_{18}	2.2%	1.00	0.94
CO_2	13.5%	6.15	6.38
H_2O	12.0%	5.45	5.75
O_2	1.0%	0.45	0
N_2	71.3%	32.42	32.42
H_2	–	–	0.27
CO	–	–	0.24
CH_4	–	–	–

can be seen that without catalyst, 6% of C_8H_{18} and ~100% of O_2 are converted, and the reaction products are CO (0.24 mol/mol C_8H_{18}), H_2 (0.27 mol/mol C_8H_{18}), CO_2 (0.23 mol/mol C_8H_{18}) and H_2O (≈0.3 mol/mol C_8H_{18}). It can be noticed that without O_2 in the gas phase, no conversion is observed, which indicates that the only reaction occurring without catalyst is an oxidation reaction. Thus the reaction products are obtained by oxidation, and as H_2/CO is equal to 1.12, it can be inferred that H_2 is produced by isooctane partial oxidation, according to the reaction (Eq. (5)):

$$C_8H_{18} + 4O_2 \rightarrow 8CO + 9H_2 \quad (5)$$

However, total oxidation also occurs since H_2O and CO_2 are produced. Some other products were also detected but in small amounts (<0.01 mol/mol C_8H_{18}), such as ethylene, propylene, isobutene and C7–C8 products.

Fig. 6 shows the typical evolution of the conversion and products distribution obtained in the presence of a Rh-supported catalyst, when the catalyst is activated in situ by reduction under hydrogen before the catalytic test. The conversion of isooctane and water is not total and decreases as a function of time-on-stream (TOS), which leads to a slight decrease in the yield of products. Moreover, as observed for blank reaction, other products, such as C2–C4 and C7–C8 hydrocarbons are produced in small amounts (<0.1 mol/mol C_8H_{18}).

When the catalyst is activated by heating up to 580 °C under the reaction conditions, i.e. in the presence of all the reactants instead of

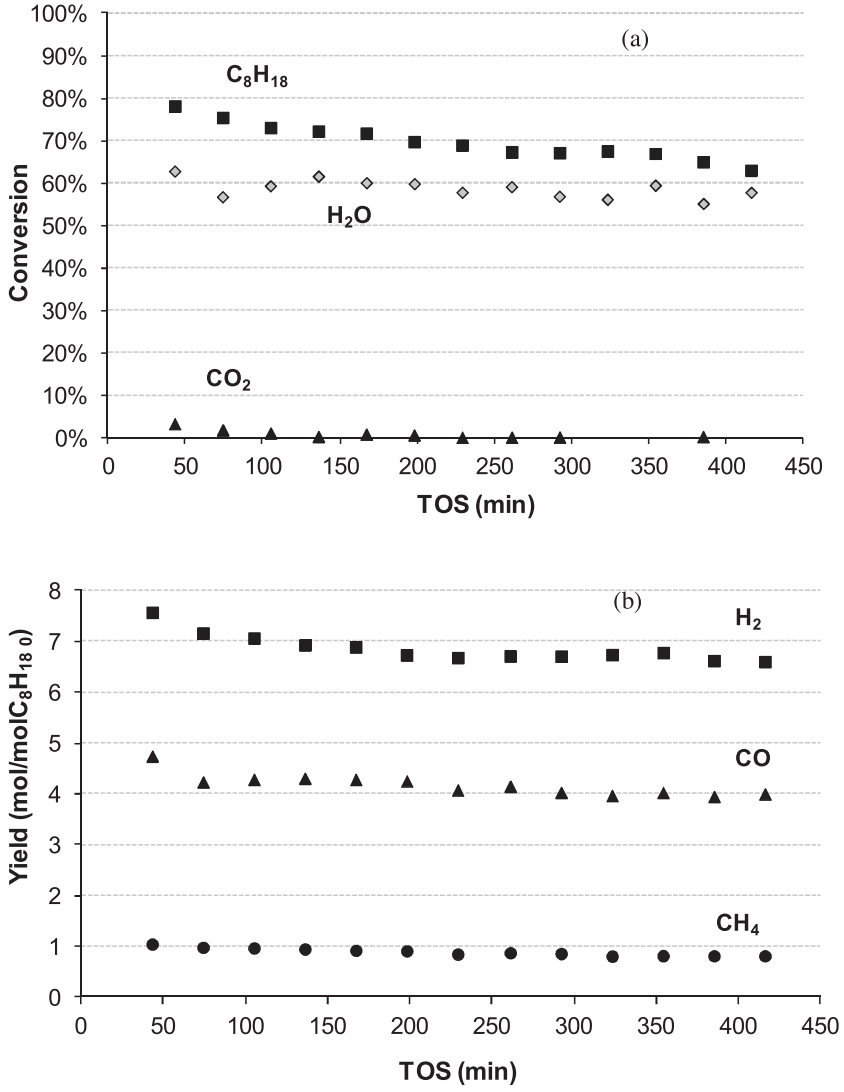

Fig. 6. Conversion of reactants (a) and products distribution (b) as a function of TOS for Rh/Al_2O_3 catalyst at 580 °C after activation under H_2.

Table 6
Effect of the pretreatment on the distribution of products and conversion of reactants after 7 h of TOS for Rh/Al_20_3 various catalysts at T = 580 °C (activation by heating under reaction conditions or under H_2).

Activation	Yield (mol/mol C_8H)			Conversion (%)		
	H_2	CO	CH_4	C_8H_{18}	H_2O	CO_2
Thermo.	7.3	6.4	2.6	100	64	16
H_2	6.6	4.0	0.82	64	57	−0.5
$C_8H_{18} + H_2O + CO_2 + O_2$	5.6	2.9	0.14	39	47	−5.0

Table 7
Distribution of products and conversion of reactants after 7 h of TOS for various catalysts at T = 580 °C, activation by heating under reaction conditions.

Catalysts	Yield (mol/mol C_8H_{18})			Conversion (%)		
	H_2	CO	CH_4	C_8H_{18}	H_2O	CO_2
Thermo.	7.3	6.4	2.6	100	64	16
Rh/CeZrAl	6.5	3.4	0.58	57	48	−0.8
Rh/Al(80)Ce(20)	6.6	3.8	0.42	53	54	1.3
Rh/Al(20)Ce(80)	6.5	3.7	0.60	54	50	−2.0
Rh/CeO_2	6.1	3.2	0.31	47	47	−2.0
Rh/Al_2O_3	5.6	2.9	0.14	39	47	−5.0

pure hydrogen, the conversion of isooctane and water is noticeably decreased (Table 6), which causes a decrease in the formation of all the products and especially H_2. This loss of performance may be due to an incomplete reduction of rhodium or to a deactivation of the catalyst that can start before the temperature of 580 °C is reached. However, as the pretreatment under reaction conditions is more realistic and closer to the REGR conditions, all the results presented hereafter were obtained after such a pretreatment.

The yields in H_2 obtained for the Rh/Al(Cex) series and for Rh/CeZrAl catalyst are reported in Fig. 7 as a function of TOS, and the complete results obtained after 7 h of TOS are summarized in Table 7. Rh/Al_2O_3 is the less efficient catalyst in terms of isooctane conversion and H_2 production. Rh/CeO_2 allows obtaining high initial yield in H_2 but deactivates rapidly. Catalysts containing Al_2O_3 and CeO_2, Rh/Al(80)Ce(20) and Rh/Al(20)Ce(80), present higher performances than Rh supported on single oxides, with an initial yield in H_2 (~6.5 mol H_2/mol C_8H_{18}) similar to the one obtained with Rh/CeO_2 but a superior stability. The addition of zirconium to the Ce-Al support improves the initial yield in H_2 (7.3 mol H_2/mol C_8H_{18}), but it decreases rapidly to reach the one observed with Al(80)Ce(20) and Al(20)Ce(80). Results summarized in Table 7 show that, whatever the catalyst, a complete conversion of isooctane is never reached and the best yields in H_2, obtained after 7 h of TOS with catalysts containing both ceria and alumina

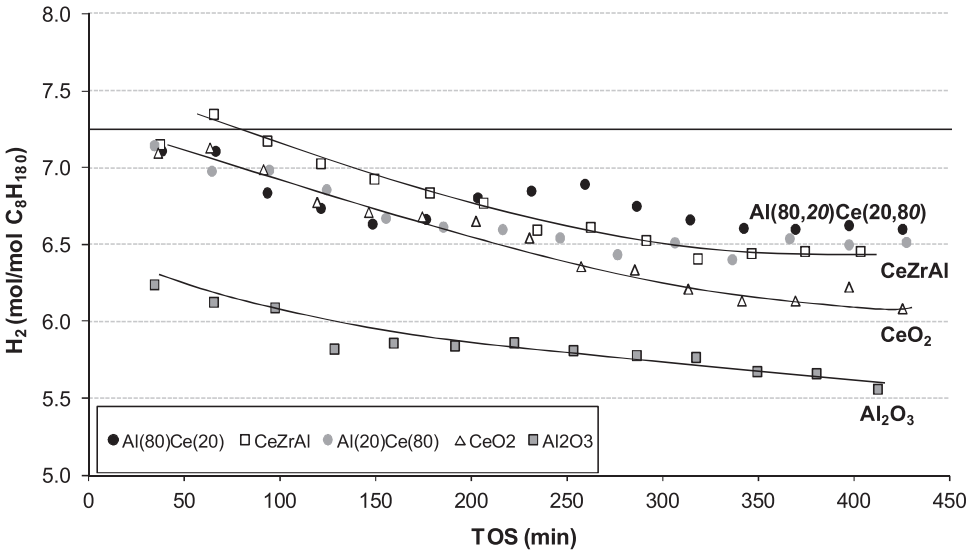

Fig. 7. Yield in H_2 as a function of TOS for Rh/Al(Cex) and Rh/CeZrAl catalysts at 580 °C after activation under reaction conditions.

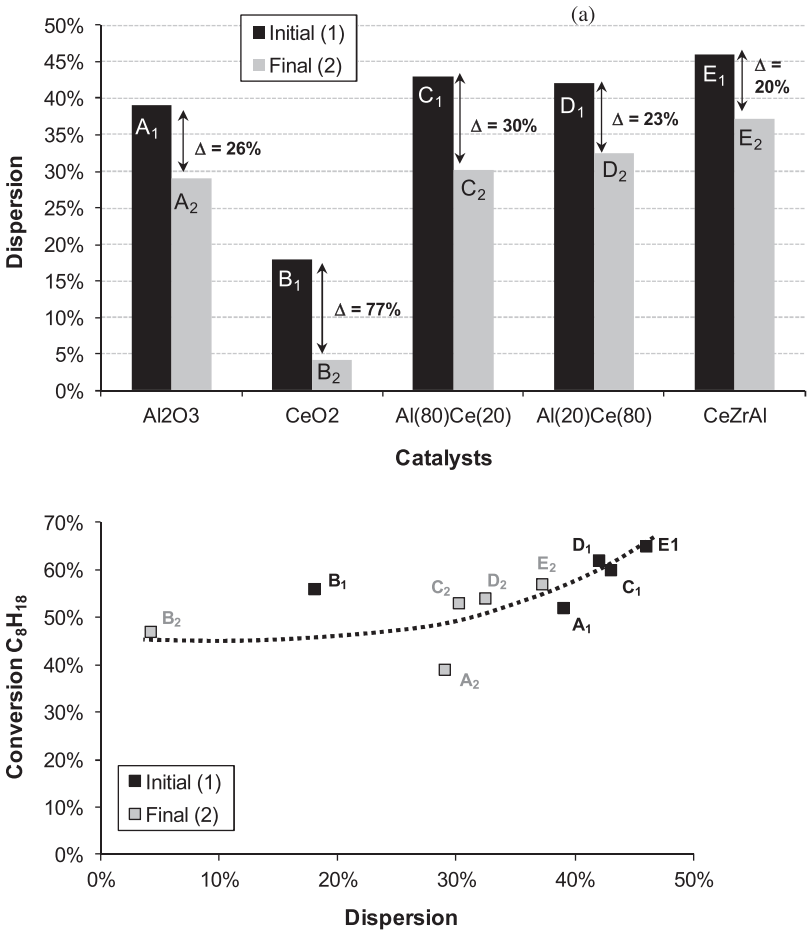

Fig. 8. Comparison of the metal dispersion of the fresh (initial: A1, B1, C1, D1 and E1) and used (final: A2, B2, C2, D2 and E2) for Rh/Al(Cex) and Rh/CeZrAl catalysts (a) and evolution of the conversion of C_8H_{18} as a function of initial and final metal dispersions.

(Rh/Al(80)Ce(20), Rh/Al(20)Ce(80), CeZrAl) are below the value predicted by calculation at the thermodynamic equilibrium. It can also be seen that the amount of methane produced is very small, much lower than the value predicted by the thermodynamic calculation. During the reaction in the REGR conditions, methane may be produced by isooctane decomposition or hydrogenolysis or by methanation of CO or CO_2 [13] and then consumed by steam or dry reforming. All these steps were studied in details in [13] and it was demonstrated that the low amount of methane is due to the limitation of its formation, isooctane decomposition and hydrogenolysis and CO_2 methanation being strongly disfavored in the reaction conditions in the presence of a Rh-based catalyst. On this type

of catalyst, methane is nearly exclusively produced by CO hydrogenation. Whatever the support, the conversion of H_2O is ~50%, whereas CO_2 conversion is ~0. One can note that a negative conversion indicates that the amount of CO_2 produced is higher than its consumption.

In order to understand the origin of the deactivation observed during the catalytic tests, the metal dispersion was evaluated at the end of the catalytic test. Results are reported in Fig. 8 where they are compared to the initial metal dispersion. It can be seen that, whatever the support, a decrease in metal dispersion is observed during the reaction. This effect is more pronounced for CeO_2, for which the metal dispersion dropped from 18% to 4% (variation $\Delta = 77\%$). Consequently, for this catalyst, the metal-support interaction is rather low and does not allow limiting the metal sintering. Supports containing mainly alumina (Al_2O_3 and Al(80)Ce(20)) present a dispersion drop of 30%, whereas those containing more ceria, Al(20)Ce(80) and CeZrAl a one of 23% (Fig. 8a). Rh sintering is probably due to the presence of steam at relatively high temperature, as proposed in [29] for $Pt/CeZrO_2$ catalyst. It can be seen from Fig. 8b that the conversion of C_8H_{18} is directly related to the metal dispersion before and after catalytic test. Although all the rhodium supports are different, the higher the metal dispersion, the higher the C_8H_{18} conversion. For this series of catalysts, the support does not play a direct role in the reaction but an indirect one, on the metal dispersion. These results also show that the deactivation may be related to the loss in metal dispersion. The effect of particle size has been demonstrated on the methane steam reforming reaction, the reaction rate per active site increasing with the dispersion on many metal catalysts, including rhodium [30]. However, an opposite result was obtained with $Ni/CeZrO_2$ for the autothermal reforming (ATR), i.e. the steam reforming in the presence of oxygen, of isooctane [31]. Indeed, it was demonstrated by varying the particle size but keeping the number of active sites constant, that the yield in CO and H_2 is higher on largest particles, which may be explained either (i) by the fact that isooctane is a large molecule needing large metal ensembles to be adsorbed or (ii) or by the ability of small Ni particles to be oxidized in the ATR conditions, leading to a loss of active sites. In fact, it was demonstrated on Ni/Al_2O_3 for isooctane conversion by partial oxidation [32] that active catalysts need to be both well dispersed and highly reducible, which are two opposite tendencies. This explanation seems valid for the Rh catalysts of the present study.

4. Conclusion

Rh catalysts supported on alumina, ceria or oxides containing both ceria and alumina were used for producing hydrogen in the presence of isooctane, used as model molecule of gasoline fuel, and various gases representative of vehicle exhaust gases. The best results in terms of conversion, stability, and yield in hydrogen were obtained on catalysts containing both ceria and alumina, namely CeO_2–Al_2O_3 (Al(20 or 80)Ce (80 or 20)) and $Ce_{0.5}Zr_{0.5}O_2$–Al_2O_3 (CeZrAl) supports. These better performances were directly linked to the higher initial Rh dispersion obtained on this type of supports as well as to the higher stability, due to lower metal sintering during the catalytic test. This metal sintering was less important for the supports containing the highest amount of cerium (Al(20)Ce(80) and CeZrAl) and the role of alumina is to improve the thermal stability of the support.

Acknowledgement

ADEME (PREDIT Program no. 06 06 C0137) is gratefully acknowledged for financial support.

References

[1] H. Wei, T. Zhu, G. Shu, L. Tan, Y. Wang, Appl. Energy 99 (2012) 534–544.
[2] Y. Jamal, T. Wagner, M.L. Wyszynski, Int J. Hydrogen Energy 21 (1996) 507–519.
[3] M.L. Wyszynski, Y. Jamal, Int. J. Hydrogen Energy 7 (1994) 557–572.
[4] S. Peucheret, M.L. Wyszynski, R.S. Lehrle, S. Golunski, H. Xu, Int. J. Hydrogen Energy 30 (2005) 1583–1594.
[5] A. Tsolakis, A. Megaritis, D. Yap, Energy 33 (2008) 462–470.
[6] A. Tsolakis, A. Megaritis, M.L. Wyszynski, K. Theinnoi, Energy 32 (2007) 2072–2080.
[7] J. Fennel, Int. J. Hydrogen Energy 39 (2014) 5153–5162.
[8] R. Stone, H.Y. Zhao, L. Zhou, SAE Technical paper No. 2010-01-0580 (2010).
[9] S. Peucheret, M. Feaviour, S. Golunski, Appl. Catal. B 65 (2006) 201–206.
[10] E. Ambroise, C. Courson, A. Kiennemann, A.-C. Roger, O. Pajot, E. Samson, G. Blanchard, Top. Catal. 52 (2009) 2101–2107.
[11] E. Ambroise, C. Courson, A.-C. Roger, A. Kiennemann, G. Blanchard, S. Rousseau, X. Carrier, E. Marceau, C. La Fontaine, F. Villain, Catal. Today 154 (2010) 133–141.
[12] S. Rijo Gomes, N. Bion, G. Blanchard, S. Rousseau, V. Bellière-Baca, V. Harlé, D. Duprez, F. Epron, Appl. Catal. B 102 (2011) 44–53.
[13] S. Rijo Gomes, N. Bion, G. Blanchard, S. Rousseau, D. Duprez, F. Epron, RSC Adv. 1 (2011) 109–116.
[14] R.M. Navarro Yerga, M.C. Alvarez-Galvan, N. Mota, J.A. Villoria de la Mano, S.M. Al-Zahrani, J.L.G. Fierro, ChemCatChem 3 (2011) 440–457.
[15] A. Holmgren, D. Duprez, B. Andersson, J. Catal. 182 (1999) 441–448.
[16] D. Andreeva, I. Ivanov, L. Ilieva, M.V. Abrashev, Appl. Catal. A 302 (2006) 127–132.
[17] J. Fonseca, S. Royer, N. Bion, L. Pirault-Roy, M.C. Rangel, D. Duprez, F. Epron, Appl. Catal. B. 128 (2012) 10–20.
[18] P. Fornasiero, R. Dimonte, G.R. Rao, J. Kaspar, S. Meriani, A. Trovarelli, M. Graziani, J. Catal. 151 (1995) 168–177.
[19] A. Tsolakis, S.E. Golunski, Chem. Eng. J. 117 (2006) 131–136.
[20] B.E. Yoldas, U.S patent 3941719 1976.
[21] S. Bernal, F.J. Botana, J.J. Calvino, M.A. Cauqui, G.A. Cifredo, A. Jobacho, J.M. Pintado, J.M. Rodriguez-Iquierdo, J. Phys. Chem. 97 (1993) 4118–4123.
[22] H.C. Yao, Y.F.Y. Yao, J. Catal. 86 (1984) 254–265.
[23] C. Leitenburg, A. Trovarelli, J. Kaspar, J. Catal. 166 (1997) 98–107.
[24] K. Otsuka, Y. Wang, M. Nakamura, Appl. Catal. A: Gen. 183 (1999) 317–324.
[25] T. Wang, L.D. Schmidt, J. Catal. 71 (1981) 411–422.
[26] H.C. Yao, H.K. Stepien, H.S. Gandhi, J. Catal. 61 (1980) 547–550.
[27] D.D. Beck, C.J. Carr, J. Catal. 144 (1993) 296–310.
[28] J. Barbier Jr., D. Duprez, Appl. Catal. B: Environ. 4 (1994) 105–140.
[29] L. Villegas, N. Guilhaume, H. Provendier, C. Daniel, F. Masset, C. Mirodatos, Appl. Catal. A: Gen. 281 (2005) 75–83.
[30] G. Jones, J.G. Jakobsen, S.S. Shim, J. Kleis, M.P. Andersson, J. Rossmeisl, F. Abild-Pederson, T. Bligaards, S. Helveg, B. Hinnemann, J.R. Rostrup-Nielsen, I. Chorkendorff, J. Sehested, J.K. Nørskov, J. Catal. 259 (2008) 147–160.
[31] J.M. Mayne, K.A. Dahlberg, T.A. Westrich, A.R. Tadd, J.W. Schwank, Appl. Catal. A: Gen. 400 (2011) 203–214.
[32] H.H. Ibrahim, P. Kumar, R.O. Idem, Energy Fuels 21 (2007) 570–580.